IEEE Access
Multidisciplinary | Rapid Review | Open Access Journal

Date of publication xxxx 00, 0000, date of current version xxxx 00, 0000.

Digital Object Identifier 10.1109/ACCESS.2017.Doi Number

Experimental Analysis of 5G NR for Indoor Industrial Environments

Berna Bulut Cebecioglu[1], Yuen Kwan Mo[2], Son Dinh-Van[2], Alex Evans[2], De Mi[1], Senior Member, IEEE, and Matthew D. Higgins[2], Senior Member, IEEE, Raouf Abozariba[1], Member, IEEE, and Adel Aneiba[1]

[1]College of Computing, Birmingham City University, Birmingham, B4 7XG, U.K.
[2]Warwick Manufacturing Group (WMG), University of Warwick, Coventry, CV4 7AL, U.K.

Corresponding author: Berna Bulut Cebecioglu (e-mail: Berna.bulut@bcu.ac.uk).

This work was supported in part by the U.K. Department for Science, Innovation and Technology (DSIT) River Severn Partnership Advanced Wireless Innovation Region, in part by the EPSRC/DSIT THRPF ORAN-TWIN project, in part by the West Midlands Innovation Accelerator WMHTIA, and in part by the Warwick Manufacturing Group (WMG) Centre High Value Manufacturing Catapult, University of Warwick, Coventry, U.K. The work of R. Abozariba was supported in part by the Department of Digital, Culture, Media, and Sport (DCMS) and Innovate U.K., under the project 5G Connected Forest (5GCF). It was also supported in part by the Local Government Association (LGA), UK, through its Digital Pathfinders Programme.

ABSTRACT Private 5G networks for industrial users are emerging as one of the leading advanced 5G use cases. This timely work presents a comprehensive experimental analysis of a private 5G network conducted in sparse and dense industrial environments at sub-6 GHz. Measured results of the over-the-air error vector magnitude (EVM) are provided, considering signal-to-noise ratio (SNR) for different 5G new radio modulation and coding schemes (MCSs), bandwidths (BWs) and numerologies (subcarrier spacings) using omnidirectional or directional antenna configurations at the transmitter (TX) and the receiver (RX). Channel sounding measurements are also conducted to characterise the channels in terms of root mean square (RMS) delay spread. The measurement results show that channels in the dense industrial environment have greater RMS delay spreads than in the sparse industrial environment due to strong reflected or scattered multipath components with significant delays. This results in higher EVMs and bit error rates (BERs), i.e., as the RMS delay spread increases, a higher SNR is required to meet the EVM limits. It is also observed that using directional antennas at the TX and RX in both environments reduces the RMS delay spread and hence the inter-symbol interference and the EVM. This allows higher MCS modes (e.g., 64 QAM and 256 QAM) to be used for reliable data transmission, significantly improving the bandwidth efficiency and reducing the latency. When evaluating system performance for different BWs and numerologies, using a lower BW and numerology provides a better system performance (lower EVMs and BERs), especially in dense industrial environments.

INDEX TERMS 5G NR, industrial environment, industrial internet of things (IIOT), measured EVM, numerology, smart factory.

I. INTRODUCTION

5G wireless access has been developed to provide enhanced mobile broadband (eMBB), massive machine-type communications (mMTC) and ultra-reliable and low-latency communications (URLLC) [1]. URLLC provides ultra-reliable, very low latency, high throughput, highly available and dependable connectivity for machine-to-machine communication, industrial automation, industrial internet of things (IIOT), digital twinning, and more in smart factory scenarios. Therefore, it is anticipated that future factories will significantly leverage the advancements facilitated by the 5G networks.

The industrial applications are time and mission-critical, and have stringent communication service availability (>99,9999%), reliability (packet error rates (PERs) 10^{-9}), latency (<1 ms), and security requirements [2], [3]. To support diverse and challenging use cases (e.g., robotic motion control, mobile collaborative cobots, remote control etc.) with extreme quality-of-service (QoS) requirements, different operation frequencies (i.e., sub-6 GHz and millimetre wave (mmWave)) and deployment scenarios, 5G new radio (NR) physical layer has been designed with a high level flexibility and scalability [4]. These include different numerology (i.e., subcarrier spacing (SS) and slot length),

bandwidth (BW), network slicing, duplexing options such as time division duplexing (TDD) and frequency division duplexing (FDD) etc. With well-designed radio network deployment and optimised configurations of the radio interface parameters, the 5G NR can provide good coverage and capacity to industrial use cases as stated in [4], i.e., 5G NR [5] can fulfil the string QoS requirements of the industrial use cases defined in [1], [2]. There is always a trade-off between system capacity and achievable performance (latency and reliability). The main challenge is to select the appropriate configuration parameters such as numerology, BW, modulation and coding schemes (MCS) according to radio channel conditions and application QoS requirements.

Factories are challenging environments in terms of radio propagation characteristics therefore in the 3rd Generation Partnership Project (3GPP) Release 15 [6] *Indoor factory* (InF) is defined as a new scenario. Factory floors are usually environments characterised as rich scattering and reflection with various metal tools, workshops/inventory areas and machines/robots, which contribute to shadowing and multipath effects. Hence, prior to the widespread deployment of 5G networks, thorough performance evaluations, testing, and optimisations are essential across various industrial scenarios. This is because industrial applications entail critical latency and reliability prerequisites.

The 5G NR performance in indoor industrial scenarios at the 4.145 GHz frequency band, corresponding to 5G NR frequency range 1 (FR1) [7] and band n77 (3300 MHz – 4200 MHz), has not yet been thoroughly investigated. This frequency band is particularly significant for the initial deployment of industrial private networks [8]. Hence, this work presents the first measured over-the-air (OTA) error vector magnitude (EVM) results, depending on signal-to-noise ratio (SNR), for various MCSs, BWs and numerologies (SSs) defined in 5G NR [5], [9]. The evaluation is conducted in two typical indoor industrial scenarios: *sparse clutter* and *dense clutter* [6], as well as in an anechoic chamber, employing both omnidirectional and directional antenna configurations. Further from the measured EVMs, the estimated bit error rate (BER) values are also calculated.

To comprehend the channel characteristics concerning delay spread and their impact on received signal quality, channel sounding measurements are also conducted in the same environments. The time dispersion nature of wireless channels is typically characterised by root mean square (RMS) delay spread, as it effectively measures multipath time dispersion and coherence bandwidth, providing insight into the potential severity of inter-symbol interference (ISI) and the required symbol length for ISI-free transmission (RMS delay spread is crucial for the wireless system design to avoid ISI) [10], [11]. Therefore, in this paper, dependencies between the RMS delay spread and EVM for different 5G NR MCS modes, BWs, numerologies and antenna configurations in indoor industrial scenarios are provided. The results presented in this work can also be used for further analysis and configuring the optimum 5G network parameters (i.e., deploying optimised 5G networks) in factory environments.

The rest of the paper is structured as follows. Section II details related works in the literature. Section III introduces the methodology used to evaluate the 5G NR performance. Section IV presents the measurement scenarios, setup and parameters. Results and analysis are provided in Section V, followed by concluding remarks in Section VI.

II. RELATED WORKS

5G NR performance for ultra-reliable machine-type communications was investigated considering the requirements for the case of factory automation in [12]. The shadow and fast fade margins required to meet the given target of 99.999% availability were provided via simulations. In [13], the required SNR versus different PER targets for a number of antenna configurations in a Rayleigh fading channel for URLLC was presented. Further latency and reliability impact on the link budget were also evaluated. In [14], latency and reliability performance for typical URLLC deployments, illustrating relevant performance metrics such as block error rate (BLER) and SNR, and involved trade-offs, were given for sparse clutter and dense clutter industrial scenarios with different transmitter (TX) heights. Simulation results showed that when TX or the receiver (RX) elevated above the clutter then the required SNR would be similar for dense and sparse environments. However, when the TX and RX were below the average height of the clutter then the required SNR in the dense environment increased. In [15], simulations were performed to evaluate different 5G NR numerology and MCS effects on the end-to-end latency and the reliability for an indoor factory scenario. The results indicated that the adaptation of MCS provided a good trade-off between throughput, latency and reliability but might not be adapted for unpredictable events such as fast-fading channels. In this case, some margins on the link budget could be more relevant. Further that it is deduced that to fulfil the requirements of the use cases defined in [2], [3] the performance of the 5G NR must be optimised. In [16], 5G radio network design options for URLLC were evaluated. The relationship between the SNR and spectral efficiency depending on the SS was provided via simulations under a fading channel. It was mentioned without any details that to achieve ultra-reliable transmissions over a fading radio channel, significant SNR margins were required. The work in [17] presented the impact of the numerology selection on the delay experienced in the radio link under line-of-sight (LOS) and non-LOS (NLOS) channel conditions in an industrial environment. Although, the simulation results indicate that a higher numerology did not always provide a lower delay; it would depend on packet size and channel conditions (i.e., under NLOS conditions, a higher SS was not always suitable), the work did not provide any detailed information on the relationship between the channel condition and the numerology.

The work in [18] conducted the OTA EVM measurements in sparse and dense industrial environments and provided the EVM values depending on the distance, and the relationships

between the EVM and RMS delay spreads for different MCS modes, directional and omnidirectional antenna configurations. Measurement results showed that in dense industrial environments the RMS delay spread could be very high (as high as 280 ns) and the higher MCS such as 64 QAM and 256 QAM were unable to meet the minimum EVM limits defined in [19]. The work limited its results to a single BW of 100 MHz and SS of 60 kHz. The related literature work in [20] performed OTA EVM measurements with varying automatic gain control, to characterise the achievable link range with 5G NR waveform at the mmWave frequency. EVM measurements were conducted in the chamber and were validated with outdoor EVM measurements with the same TX power level. Results showed that OTA EVM measured in the chamber correlated well with LOS outdoor measurements. It was further indicated that the EVM provided a more consistent measure of RF performance than BER or BLER. The work neither considered industrial scenarios nor the 5G NR parameters such as numerology, BW or different antennas.

In [21], the relation between optical SNR, EVM, and BER was investigated. Theoretical results and numerical simulations were compared to measured values of optical SNR, EVM, and BER. Results confirmed experimentally and by simulations that the BER could be estimated from measured EVM data by an analytic relation. Similarly, the relationship between the EVM and BER was provided only for different MCS modes in [22]-[30]. In [31], the performance of 5G in terms of latency, reliability, and throughput in the InF sub-scenarios defined by the 3GPP was evaluated considering different user speeds, packet sizes and frequency bands. For a specific configuration, for example, BW and SS, it was investigated via simulations whether the 5G NR could fulfil the QoS requirements for massive wireless sensor networks, autonomous mobile robots, and augmented reality applications. None of these literature works has ever investigated the 5G NR performance in different real-world industrial environments and provided the relationship between the EVM and SNR for different MCS modes, SSs (numerologies), BWs, and antenna configurations which is the aim of this paper. As stated in [32], more in-depth research is needed to address these research gaps and challenges in industrial environments.

III. ANALYSIS METHODOLOGY

Difference between the measured carrier signal and the reference signal can be presented by the EVM which is used to define a modulation quality [2]. EVM is a measure of the difference between the ideal symbols, *I(t, f)*, and the measured symbols, $Z'(t,f)$ at the *f*-th sub-carrier and *t*-th symbol, after the equalisation, and must be calculated for each NR carrier over all allocated resource blocks (RBs) and downlink subframes as follows [19]:

$$EVM = \sqrt{\frac{\sum_{t\in T}\sum_{f\in F(t)}|Z'(t,f)-I(t,f)|^2}{\sum_{t\in T}\sum_{f\in F(t)}|I(t,f)|^2}} \quad (1)$$

where *T* is the number of symbols over which the EVM is measured, and *F(t)* is the number of subcarriers within the RBs with the considered modulation scheme being active in symbol *t*.

Larger EVM values indicate a greater distance between the measured and the ideal symbols thus leading to a higher probability of bit errors. The value of the EVM is averaged over a large set of symbols and given as the RMS value of the errors between a collection of measured symbols and ideal symbols. For a TDD transmission it is defined as [19]:

$$EVM_{RMS} = \sqrt{\frac{1}{\sum_{i=1}^{N_{dl}^{TDD}} N_i}\sum_{i=1}^{N_{dl}^{TDD}}\sum_{j=1}^{N_i} EVM_{i,j}^2} \quad (2)$$

where N_{dl}^{TDD} is the number of slots with downlink symbols within a 10 ms measurement interval and N_l is the number of resource blocks with the considered modulation scheme in slot *i*. The EVM_{RMS} is expressed in percentage (%) or in decibel (dB).

For each modulation, used in the 5G NR, there is a defined EVM limit, for which the transmitted signal has an acceptable quality (the lower the EVM, the better the signal quality). Table 1 provides the EVM limits in percentage and dB depending on the MCSs defined in the 5G NR standard [19]. When the modulation order is increased (throughput is also increased), the required EVM limit reduces. Since closer the symbols are to each other in the constellation, a lower EVM is required for achieving decent BER in the RX.

EVM is an effective method of evaluating overall 5G NR system performance and QoS. It enables analysis of the effect of various nonidealities and distortions in the transceiver and the radio propagation channel such as noise, ISI, and nonlinearity. Unlike the commonly used figure of merits such as BER, which gives a simple one-to-one binary decision as to whether a bit is erroneous or not and does not provide any information about the reason for the distortions in the communication systems, EVM measurements allow precisely determining the cause of errors and their effects on the communication systems [26], [33].

In literature [22], [23], it is shown that EVM can be related to other performance metrics such as SNR and BER. Since EVM measurements can be obtained by using a vector signal generator (VSG) and a signal and spectrum analyser (SSA), reusing already available EVM measurements to infer more information on the communication system could reduce the system complexity by eliminating the need to have separate modules to estimate or measure other useful metrics [23]. If the received signal is only impaired by additive white Gaussian noise (AWGN) then the EVM_{RMS} can be related to the SNR and calculated as [22], [23]:

$$EVM_{RMS} \approx \sqrt{\frac{1}{SNR}} \quad (3)$$

SNR is defined as the ratio of the received signal power to the noise power within the bandwidth of the transmitted signal. The received power is determined by the transmitted power and the path loss (shadowing and multipath fading). The noise power is determined by the BW of the transmitted signal and the spectral properties of the noise [10]. In AWGN, the BER depends on the received SNR and hence EVM_{RMS} and can be approximated from the measured EVM_{RMS} values as follows [22]:

$$BER \approx \frac{2\left(1-\frac{1}{L}\right)}{\log_2 L} Q\left[\sqrt{\left[\frac{3\log_2 L}{L^2-1}\right]\frac{2}{EVM_{RMS}^2 \log_2 M}}\right] \quad (4)$$

where L is the number of levels in each dimension of the M-ary modulation system, $Q[.]$ is the Gaussian co-error function.

In a fading environment, the received signal power (and hence SNR) varies randomly over distance or time as a result of shadowing and/or multipath fading. The performance metric depends on the rate of change of the fading when SNR is random. In [23], the relationship between EVM_{RMS} and SNR is provided for fading channels. However, for high SNR values and higher modulation orders, the approximation of the EVM_{RMS} value in (3) can be used. Therefore, in this work, the measured EVM values are used in (4) to estimate the BER for different industrial environments (channels).

TABLE 1
EVM LIMITS DEPENDING ON THE MCS DEFINED IN [19]

MCS	Required EVM (%)	Required EVM (dB)
16 QAM	13.5	-17.39
64 QAM	9	-20.92
256 QAM	4.5	-26.94

IV. MEASUREMENT SCENARIOS AND SETUP

A. MEASUREMENT SCENARIOS

3GPP standard (TR 38.901, Release 16) [6] defines two indoor scenarios for industrial applications: *sparse clutter* and *dense clutter*, based on the density levels of "clutter", such as machinery, assembly lines, storage shelves. As stated in 3GPP standard [6], the *sparse clutter* scenario may encompass large machines with regular metallic surfaces, found in mixed production areas with open spaces and storage/commissioning areas. On the other hand, the *dense clutter* scenario may involve small to medium metallic machinery and objects with irregular structures, typical of assembly and production lines surrounded by various small-sized machines. To evaluate the 5G NR performance in different real-world industrial environments, the measurements provided in this work were performed at the University of Warwick, UK, in the Digital Automation Laboratory (DAL), representing a *sparse clutter*, the International Manufacturing Centre (IMC) Hall, representing a *dense clutter* indoor industrial scenario, and an anechoic chamber in which there is no multipath and interference thus represents an AWGN scenario as seen in Fig. 1a-c. The AWGN channel is also important for providing an upper bound on system performance. The DAL measures 29.5 meters in length, 7 meters in width, and 7.5 meters in height. As shown in Fig. 1b, it contains several large industrial machines with metal or metal surfaces, alongside open areas and storage facilities. The DAL is enclosed by a concrete wall on one side and glass windows on the other. On the other hand, the IMC Hall is densely packed with numerous industrial machines, along with some workshop areas. The machines in the IMC Hall are surrounded by cages consisting of metal surfaces and glass windows as shown in Fig. 1c. The dimensions of the IMC Hall are 68 meters in length, 25 meters in width, and 14.6 meters in height. The anechoic chamber`s dimensions are 9 m in length, 9 m in width and 2.8 m in height.

In all three scenarios, the TX and the RX were mounted on the non-reflective poles as seen in Fig. 1a-c, with heights set at 2 meters and 1.5 meters above ground level, respectively. The height of the RX was chosen to approximate the height of wireless terminals typically mounted on machinery or robot arms. On the TX side, a directional antenna with 11 dBi gain was utilised for all measurement campaigns. On the RX side, both directional and omnidirectional antennas were employed, with gains of 11 dBi and 3 dBi, respectively. This setup allowed for EVM measurements to be conducted for directional-to-directional and directional-to-omnidirectional antenna pairs. During all measurements, the TX and RX locations were fixed and had a separation distance of 5 m. As shown in Figs. 1a-c that for all measurement scenarios, the TX and RX locations had a clear optical path to one another, thus representing an LOS environment. Additionally, all OTA EVM measurements were carried out during slow work periods to minimise exposure to external factors.

B. MEASUREMENT EQUIPMENT

In this work, the measurements were performed by using Rohde & Schwarz (R&S) 5G NR equipment which consists of an R&S SMBV100B VSG, and an R&S FSVA3007 SSA. In indoor measurement setups, the VSG and SSA are connected via two cables. These cables serve the purpose of synchronising the transmitter and the receiver by utilising a reference frequency and transmitting the trigger signal.

5G NR operation bands were divided into two groups, namely, FR1 [7] and frequency range 2 (FR2) [34]. FR1 covers the spectrum from 410MHz to 7.125 GHz, while FR2 spans from 24.25 GHz to 52.6 GHz. Each frequency range is further divided into NR bands with different SS, channel BW and duplexing options such as TDD and FDD. In this work, the carrier frequency, f_c, of 4.145 GHz was utilised. This frequency corresponds to 5G NR band n77 (3300 MHz – 4200 MHz) [7]. It is important to note that during the measurements, there were no active interfering wireless systems operating in these frequency bands.

The VSG was configured according to the test models (TMs) specified in [5], [19], which are based on the 5G NR Release15 downlink specifications. EVM measurements were

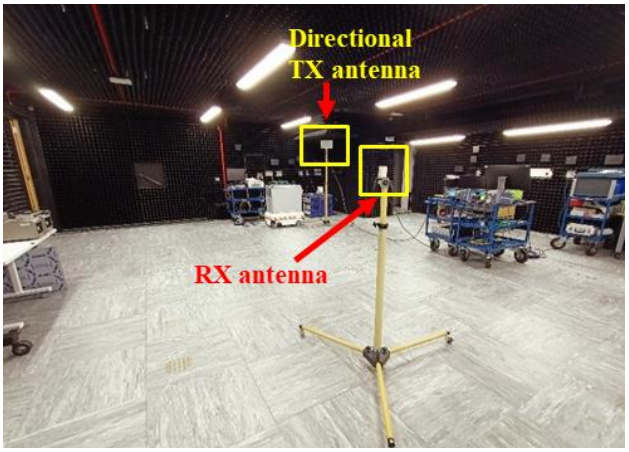

(a) Anechoic Chamber

(b) Digital Automation Laboratory (DAL)

(c) International Manufacturing Centre (IMC) Hall

FIGURE 1. Measurement scenarios (a) Anechoic Chamber, (b) Digital Automation Laboratory (DAL) and (c) International Manufacturing Centre (IMC) Hall.

conducted for 16 QAM, 64 QAM and 256 QAM modulation schemes (i.e., TMs) using an SS of 30 and 60 kHz, a channel BW of 50 and 100 MHz with the TDD transmission scheme.

To characterise the channels, channel sounding measurements were also conducted for the same scenarios where the EVM measurements were performed. The detailed information on the channel sounding process can be found in our previous work [18]. Table 2 summarises the parameters used for the channel sounding and the OTA EVM measurements of the 5G NR signals. At the RX side (i.e., in the SSA), the same TMs and configurations were replicated to demodulate the received 5G NR signals and calculate the EVM. To evaluate the EVM performance of the 5G NR, the transmit power was set to 10 dBm and the SNR was changed from 18 dB to 45 dB. In the VSG the transmit power was fixed to 10 dBm and hence at the RX (in the SSA), the received power was fixed. Therefore, in order to change the SNR value, the noise level (power) was changed in the VSG.

TABLE 2
PARAMETERS USED IN VSG AND SSA FOR CHANNEL SOUNDING AND OTA EVM MEASUREMENTS

Parameter	Value
Channel sounding	
Carrier frequency, f_c	4.145 GHz
Bandwidth, BW	300 MHz
Transmit power at TX, P_t	20 dBm
TX height	2 m
RX height	1.5 m
Directional TX antenna gain, G_t	11 dBi
Directional RX antenna gain, G_r	11 dBi
Omnidirectional RX antenna gain, G_r	3 dBi
Cable loss, L_c	8 dB
OTA EVM	
Bandwidth, BW	50 MHz, 100 MHz
Transmit power at TX, P_t	10 dBm
SS	30 kHz (μ=1), 60 kHz (μ=2)
MCS	16 QAM, 64 QAM and 256 QAM
Duplexing	TDD

Flexibility is provided to adjust the radio interface by selecting the appropriate numerology (represented as μ)/waveform that caters to the specific radio channel characteristics. These flexible numerologies contribute to enhancing the overall achievable spectrum efficiency. In the case of the 5G NR operating band n77 for FR1, 15 kHz, 30 kHz and 60 kHz SS are permitted. Table 3 presents the SS, orthogonal frequency division multiplexing (OFDM) symbol duration T_S, cyclic prefix (CP) duration T_{CP}, slot duration, number of OFDM symbols and maximum allocated BW options of the 5G NR defined in [5], [9].

TABLE 3
5G NR NUMEROLOGY

μ	SS (kHz)	T_S (µs)	T_{CP} (µs)	Slot duration (ms)	# of OFDM symbols in one slot	Max. BW (MHz)
0	15	66.67	4.76	1	14	50
1	30	33.33	2.38	0.5	14	100
2	60	16.67	1.19|4.17	0.25	12|14	100

V. RESULTS AND ANALYSIS

In this section, first, the measured EVM versus SNR values in the anechoic chamber, sparse and dense industrial environments for different MCSs, SSs, BWs and antenna configurations are presented. Then, BER versus SNR values calculated from the measured EVMs are provided.

A. EVM VERSUS SNR RESULTS

Fig. 2-4 show the measured EVM versus SNR values depending on the SSs, BWs and antenna configurations in the anechoic chamber, DAL (sparse) and IMC Hall (dense) for 16 QAM, 64 QAM and 256 QAM respectively. As mentioned before, the measurements conducted in the chamber present the system performance under the AWGN channel, which presents no fading and/or interference and also provides an upper bound on system performance. The physical size and type of construction materials used for the indoor industrial scenarios affect multipath delay spread and the consequent frequency selective fading. To characterise the channels (fading properties) in the DAL and IMC Hall, the channel sounding was performed for the same EVM measurement scenarios. The RMS delay spreads calculated in DAL are 56.46 ns and 42.35 ns for omnidirectional and directional antennas respectively whereas, in IMC Hall RMS delay spreads are 146.52 ns and 132.58 ns for omnidirectional and directional antennas respectively. It is expected that using the directional antennas at the TX and RX reduces the time dispersion in the channel thus providing lower RMS delay spread since directional antennas suppress most of the major multipath signal components outside of the main beamwidth [35]. However, in dense industrial environments, where there are many metallic objects/tools and surfaces, using directional antennas may result in a larger RMS delay spread compared to the omnidirectional antennas as observed in [18]. This is because, in dense industrial environments, the strong reflected and scattered paths received from the metallic objects and surfaces have large delay differences with the strongest signal, which results in large RMS delay spread values. The RMS delay spreads in the dense environment (in IMC Hall) are almost three-fold higher than in the sparse environment (in DAL). Therefore, in industrial environments, the RMS delay spread strongly depends on the objects around the TX and RX, and the antenna patterns used at the TX and RX.

When the EVM versus SNR is investigated, it can be seen that increasing the SNR results in a decrease in the measured EVM values due to the lower noise level (vector). The effect of antenna configuration on the EVM for the same SNR is clearly visible, i.e., for the same SNR using a directional antenna provides lower EVMs than using an omnidirectional antenna at the RX. Especially, using the omnidirectional antenna in a dense industrial environment (in IMC Hall) results in very poor system performance (higher EVMs) for the same SNR values. This is attributed to the higher RMS delay spread due to frequency selective fading which gives rise to ISI and thus causes an irreducible EVM floor in the measured EVM values, i.e., the larger the RMS delay spread higher the EVM values. As seen in Fig. 2c- 4c that increasing SNR does not reduce the EVM. For the highest SNR value of 45 dB, the lowest EVM value can be around -35 dB. However, for the same SNR (45 dB) the lowest EVM value can be

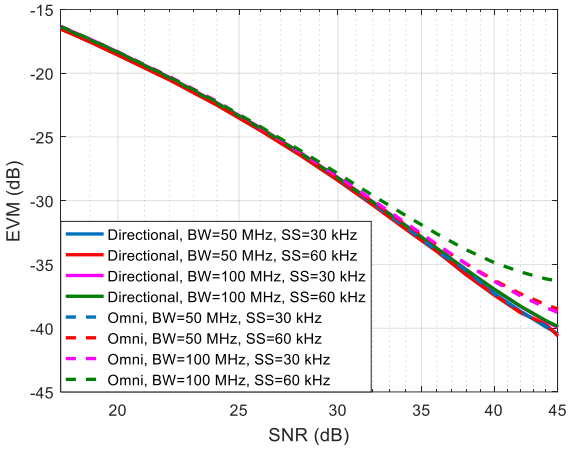

(a) EVM vs. SNR in the Chamber

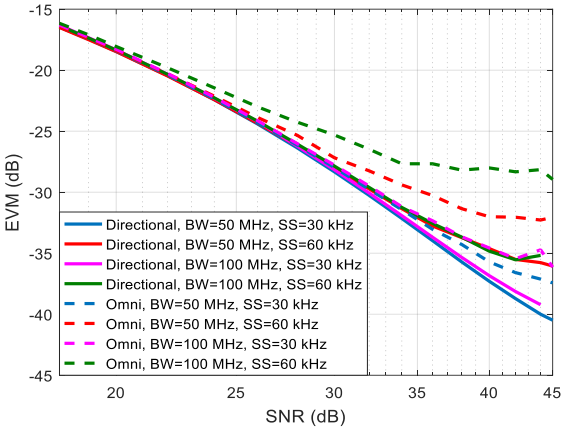

(b) EVM vs. SNR in DAL

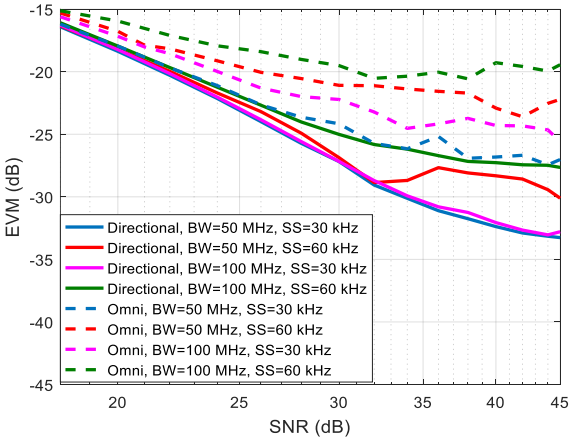

(c) EVM vs. SNR in IMC Hall

FIGURE 2. Measured EVM versus SNR depending on the BW, SS and antenna configurations (directional and omnidirectional) for 16 QAM: (a) in the Chamber, (b) in DAL and (c) in IMC Hall.

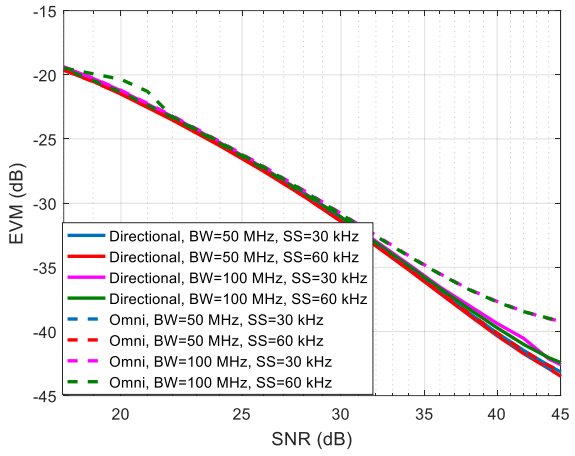

(a) EVM vs. SNR in the Chamber

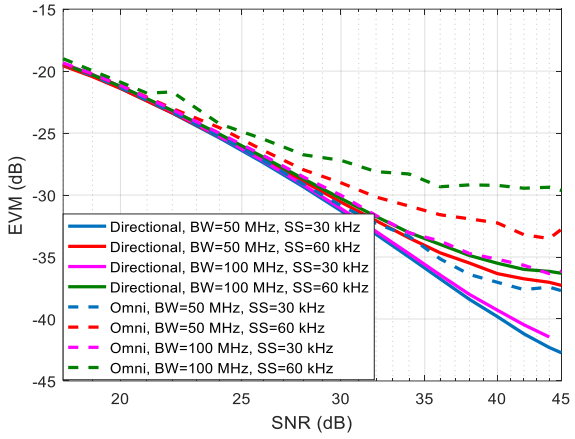

(b) EVM vs. SNR in DAL

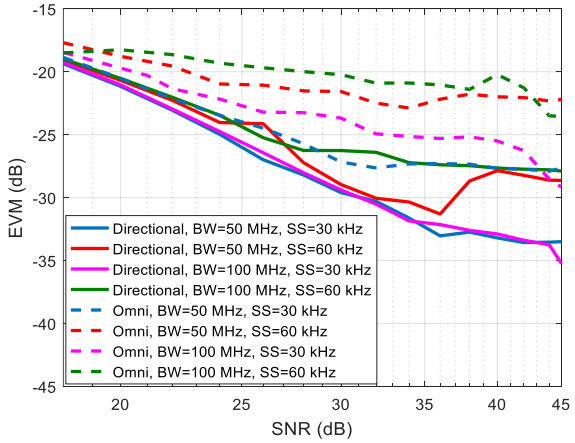

(c) EVM vs. SNR in IMC Hall

FIGURE 3. Measured EVM versus SNR depending on the BW, SS and antenna configurations (directional and omnidirectional) for 64 QAM: (a) in the Chamber, (b) in DAL and (c) in IMC Hall.

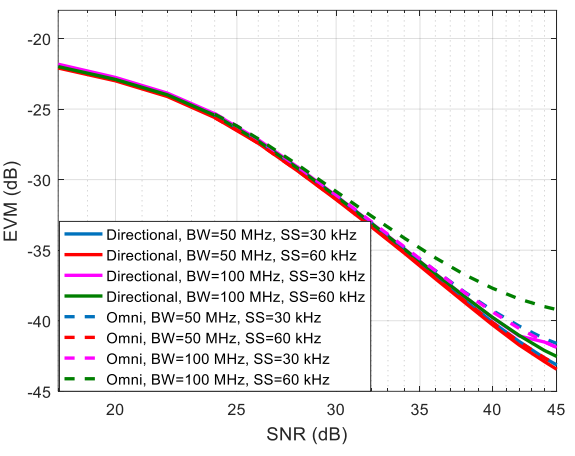

(a) EVM vs. SNR in the Chamber

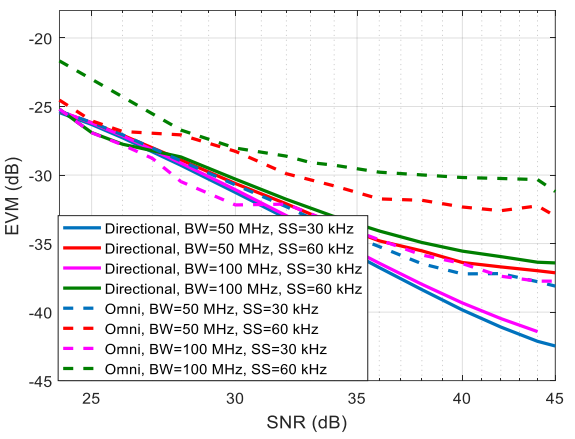

(b) EVM vs. SNR in DAL

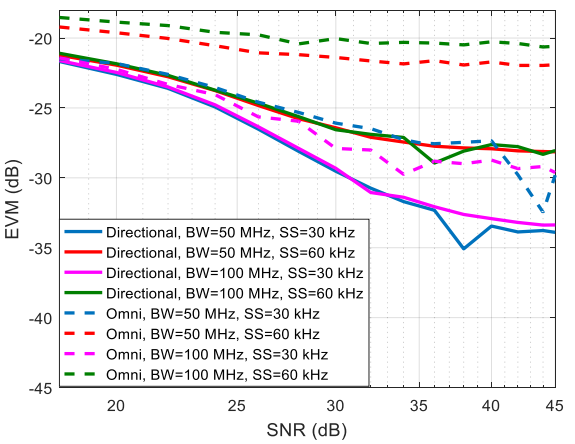

(c) EVM vs. SNR in IMC Hall

FIGURE 4. Measured EVM versus SNR depending on the BW, SS and antenna configurations (directional and omnidirectional) for 256 QAM: (a) in the Chamber, (b) in DAL and (c) in IMC Hall.

as low as -43 dB in the chamber and the sparse industrial environment (in DAL). When MCS modes are compared, it is seen that the EVM increases for the large modulation order due to the high noise sensitivity of the high order MCSs.

Higher MCS modes (i.e., 64 QAM and 256 QAM) require higher SNR to provide acceptable EVM results compared to the lower MCS modes (such as 16 QAM). Moreover, to meet the EVM limits for the MCSs defined in Table 1 [19],

TABLE 4
MINIMUM REQUIRED SNRS TO MEET THE EVM LIMITS FOR EACH MCS MODE IN DIFFERENT ENVIRONMENTS

Scenario	MCS	Required SNR (dB)							
		Directional, BW=50 MHz, SS=30 kHz (μ=1)	Directional, BW=50 MHz, SS=60 kHz (μ=2)	Directional, BW=100 MHz, SS=30 kHz (μ=1)	Directional, BW=100 MHz, SS=60 kHz (μ=2)	Omni, BW=50 MHz, SS=30 kHz (μ=1)	Omni, BW=50 MHz, SS=60 kHz (μ=2)	Omni, BW=100 MHz, SS=30 kHz (μ=1)	Omni, BW=100 MHz, SS=60 kHz (μ=2)
Chamber	16 QAM	19	19	19	19	19	19	19	19
	64 QAM	19.5	19.5	19.5	19.5	19.5	19.5	19.5	20.5
	256 QAM	26	26	26	26	26	26	26	26
DAL	16 QAM	19	19	19	19	19	19	19	19.1
	64 QAM	19.8	19.8	19.8	19.8	19.8	19.8	19.8	20
	256 QAM	25.7	25.7	25.7	25	25.7	26.5	25	28.5
IMC Hall	16 QAM	19.3	19.3	19.3	19.6	19.6	20.7	20.5	24
	64 QAM	19.8	20.5	19.8	20.5	20.5	24	21.8	34
	256 QAM	26.5	32	26.5	32	33	-	28.5	-

omnidirectional RX requires higher SNR than the directional. The required SNR is dramatically increased especially for the dense industrial environment and higher MCS modes such as 64 QAM and 256 QAM. In practical communication systems, in order to increase the SNR, TX power must be increased. However, it is not desired and always possible to increase the TX power since there are limitations/regulations on the maximum TX power. Considering all measurement results it is recommended to use directional antennas at the TX and RX, especially in the dense industrial environments where the RMS delay spread due to metallic surfaces may be higher than the symbol duration.

When the system performance is evaluated for different BW and SS, it is shown that under an ideal channel condition (i.e., AWGN channel) as seen in Fig. 2a- 4a, using the directional antenna at the RX can provide up to 4 dB lower EVMs compared to the omnidirectional antenna. Performance differences get higher under fading channels as seen in Fig. 2b- 4b for the sparse (DAL) and in Fig. 2c- 4c for the dense (IMC Hall) industrial environments where the differences between the measured EVMs depending on the antenna configuration, BW and SS are as high as 12 and 14 dB respectively. It is seen that under non-ideal channel conditions (in DAL and IMC Hall) using lower BW and SS (i.e, BW=50 MHz and SS=30 kHz) provide the best system performance (meets the minimum EVM limit with the lowest SNR value) while higher BW and SS (i.e, BW=100 MHz and SS=60 kHz) provide the worst performance irrespective of antenna configurations and MCS modes. It is also observed that for SS=30 kHz, using 100 MHz BW provides almost the same performance (EVM versus SNR) as the 50 MHz BW. Further in the dense industrial environment, the 256 QAM with 60 kHz SS is unable to fulfil the required EVM limit of -26.94 dB when the omnidirectional antenna is used at the RX. It is apparent that the value of the SS dominates the system performance most compared to the BW under nonideal channel conditions (lower the SS lowers the required SNR for meeting the EVM limits). It is further observed that higher SSs (thus shorter symbol durations and CPs) are far more vulnerable to ISI in indoor factory environments and increasing the SNR does not reduce the EVM. Therefore, for applications which require higher data rates and reliable data delivery, it is recommended to use the 50 MHz BW, 30 kHz SS and directional antennas at the TX and RX. However, for the AWGN channel (in Fig. 2a- 4a), the system performance mostly depends on the BW, i.e., higher BW provides higher EVM results (poor system performance). This is expected since the noise power depends on the BW of the TX signal. It is worth mentioning that for time-critical manufacturing applications (e.g., robotic motion control) using shorter symbol duration (higher SS) is desired to meet the required QoS demands in terms of latency, in this case, a higher SS (e.g., 60 kHz) can be used at the expense of the higher TX power.

Table 4 presents the minimum required SNR values that provide the EVMs equal or below the limits provided in Table 1 for different environments, MCS modes, BWs, SSs and antenna configurations. These results provide valuable insights on the 5G NR network configuration parameters that can be selected for different manufacturing applications depending on their QoS requirements.

B. BER VERSUS SNR RESULTS

BER versus SNR is one of the most popular figures of merits that is used to evaluate the performance (QoS) of communications systems. In the 5G NR different applications have different QoS (BER, PER, BLER etc.) requirements. Therefore, for each MCS mode the required SNR must be defined considering the application`s QoS requirements. With this regard, it is paramount to estimate the BER from the measured EVM values. To this end, Fig. 5a-f show the estimated BERs from the measured EVMs depending on the SNR for different MCS modes, BWs, SSs, antenna configurations and environments (channels).

As expected in the Chamber the BER performance depending on the SNR thus does not change much. However, in DAL and IMC Hall random nature of the fading mechanism (the vector addition of all multipath signals) results in dynamic changes to the BER. It is seen that substantial changes in the BER are observed depending on the MCS mode, SS and BW

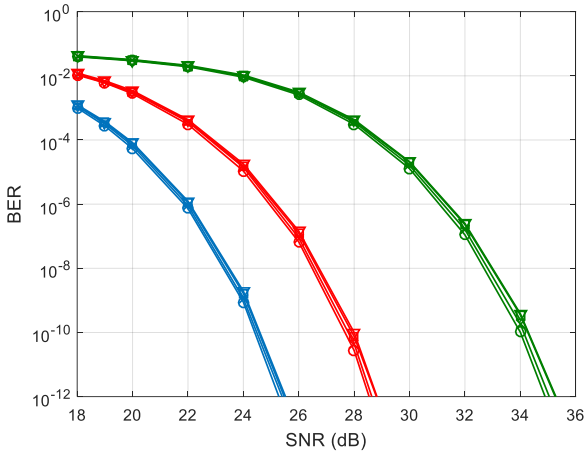

(a) BER vs. SNR with a directional RX antenna in the Chamber

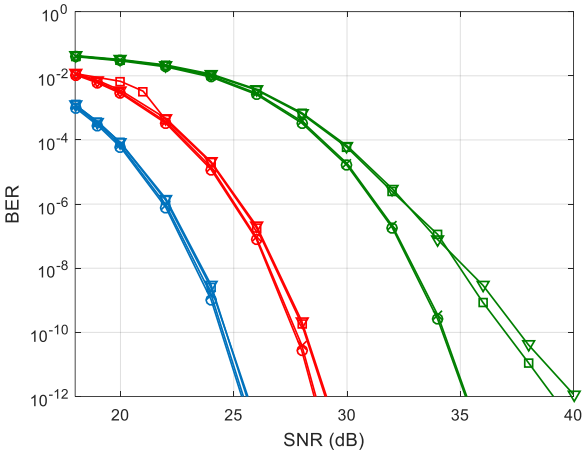

(b) BER vs. SNR with an omnidirectional RX antenna in the Chamber

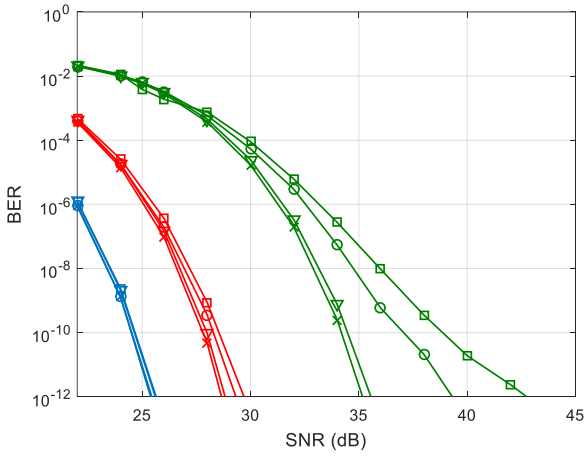

(c) BER vs. SNR with a directional RX antenna in DAL

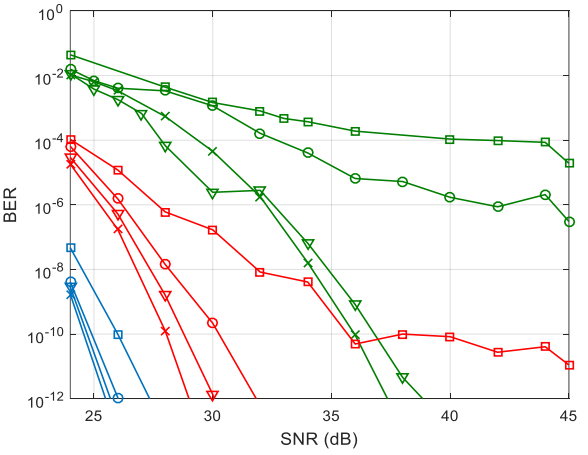

(d) BER vs. SNR with an omnidirectional RX antenna in DAL

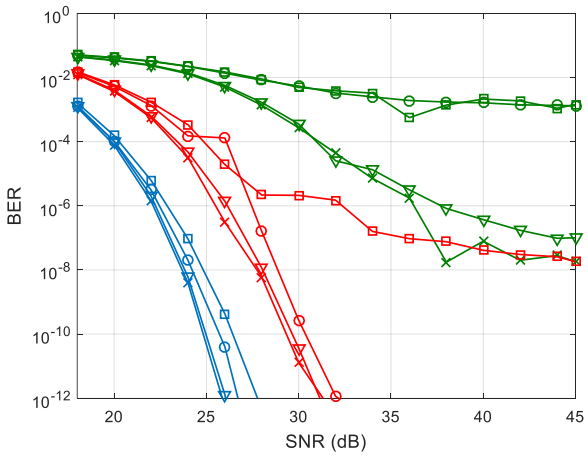

(e) BER vs. SNR with a directional RX antenna in IMC Hall

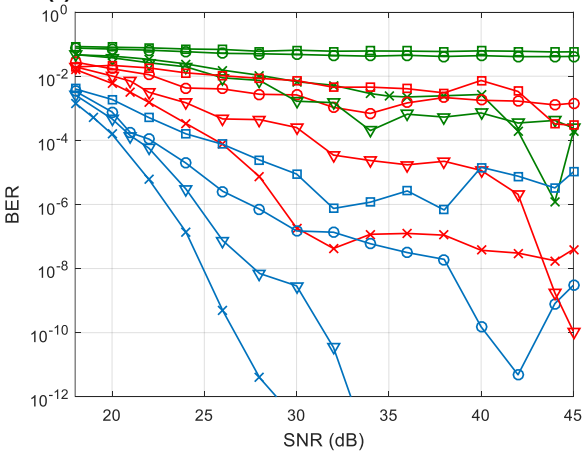

(f) BER vs. SNR with an omnidirectional RX antenna in IMC Hall

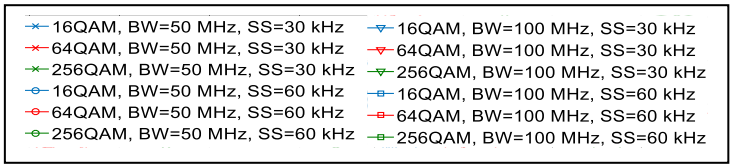

FIGURE 5. **Estimated BER versus SNR depending on the MCS mode, BW and SS: (a) with a directional RX antenna in the Chamber, (b) with an omnidirectional RX antenna in the Chamber, (c) with a directional RX antenna in DAL, (d) with an omnidirectional RX antenna in DAL, (e) with a directional RX antenna in IMC Hall and (f) with an omnidirectional RX antenna in IMC Hall.**

configurations when the omnidirectional antenna is used at the RX in DAL and IMC Hall. Using directional antenna at the TX and RX can provide less varying BER performance than using omnidirectional antennas as seen in Fig. 5c-f thus providing robust data transmission. It is clear that using directional antennas at the TX and RX enables accurate estimation of the MCS mode for the next data transmission depending on the SNR. This makes the signal processing and link adaptation algorithms to be less complex. However, using the omnidirectional antenna at the RX makes the communication systems sensitive to the selected BW, SS and MCS modes.

In Fig. 5d-f, it is seen that under fading channels, using higher MCS modes such as 64 QAM and 256 QAM with the higher SS causes poor system performance (irreducible BER floors occur at very high SNRs). For example, considering the scenario in Fig. 5f when an application has an acceptable BER of 10^{-6}, in this case only the lowest MCS of 16 QAM and the 64 QAM with the lower SS can be selected for data transmission since other configurations are unable to meet the required BER limit. Additionally, for the same SS, using a higher BW results in a higher BER since increasing the BW leads to higher receiver sensitivity. In order to use higher MCS modes (256 QAM) for data transmission, which reduces the bandwidth demand, using directional antennas at the TX and RX, and lower SS and BW are required.

VI. CONCLUSION

This paper provided an experimental analysis of the 5G NR performance for indoor factory scenarios at 4.145 GHz. Measured OTA EVM results with respect to SNR were reported for different 5G NR MCS modes, BWs and numerologies in sparse, dense industrial environments, and an anechoic chamber using omnidirectional and directional antenna configurations at the TX and RX. To define the propagation effects on the system performance, the channel sounding measurements were also conducted in the same environments, yielding insight into the time dispersion characteristics of the channels. From the measurements results and analysis, it was observed that channels in the dense industrial environment had greater RMS delay spreads due to strong reflected and scattered signals received from the metallic objects and surfaces, and hence higher EVMs than in the sparse industrial environment. The RMS delay spreads in the dense environment (in IMC Hall) were almost three times higher than in the sparse environment (in DAL). Using directional antennas at the TX and RX in both environments would reduce the RMS delay spread (and hence ISI) and thus the EVM. As a result of that higher MCS modes (64 QAM and 256 QAM) can be selected for data transmission which significantly improves the bandwidth efficiency and reduces the latency. However, when omnidirectional antennas were used increasing the SNR did not reduce the EVM, especially for higher order MCS modes in the dense industrial environment, i.e., irreducible EVM floors were observed due to ISI.

When the effects of the selected BW and SS on the system performance were evaluated, it was shown that the system performance was mostly dominated by the SS under fading channels, i.e., using lower SS (higher symbol and CP lengths) provided lower EVM results. Although 5G NR proposed higher SS to provide low latency communication, it was shown that severe multipath effects observed in industrial environments (especially the dense environment) limit the selection of the higher SS as well as higher MCS modes for data transmission. The results further indicate that using directional antennas at the TX and RX overcomes these limitations, enables using higher MCS modes and SS (numerology) and thus provides higher throughput and lower delay.

The measured OTA EVM results for different MCS modes, BWs, SSs and antenna configurations presented in this work will provide invaluable insight into the 5G NR private network performance deployed in sparse and dense factory environments (under different channel conditions). These results can be used for developing link adaptation algorithms and optimising the network performance in order to meet the QoS requirements of the industrial applications. One of the future works can be performed to analyse the system performance for different BWs, SSs and MCS modes considering the latency and reliability QoS requirements of the application(s). Further work is also needed to evaluate system performance and provide results for NLOS scenarios, as our current work is limited to LOS scenarios only.

REFERENCES

[1] 3GPP. Study on Scenarios and Requirements for Next Generation Access Technologies (Release 17). 3GPP TR 38.913 V17.0.0, March 2022.
[2] 3GPP. Study on Communication for Automation in Vertical domains (Release 16). 3GPP TR 22.804 V16.3.0, July 2020.
[3] G. Hampel, C. Li and J. Li, "5G Ultra-Reliable Low-Latency Communications in Factory Automation Leveraging Licensed and Unlicensed Bands," in *IEEE Communications Magazine*, vol. 57, no. 5, pp. 117-123, May 2019.
[4] 5G-SMART, "Radio network deployment options for smart manufacturing," deliverable D1.4, Nov. 2021, [Online]. Available: https://5gsmart.eu/wp-content/uploads/5G-SMART-D1.4-v1.0.pdf.
[5] 3GPP. NR; Base Station (BS) radio transmission and reception (Release 17). 3GPP TS 38.104 V17.6.0, June 2022.
[6] 3GPP. Technical specification group radio access network; study on channel model for frequencies from 0.5 to 100 GHz (Release 17). TR 38.901 V17.0.0, March 2022.
[7] 3GPP. Technical Specification Group Radio Access Network; NR; User Equipment (UE) radio transmission and reception; Part 1: Range 1 Standalone (Release 18). TS 38.101-1. V18.2.0, June 2023.
[8] 3GPP. Scenarios, Frequencies and New Field Measurement Results from two Operational Factory Halls at 3.5 GHz for various Antenna Configurations. Nokia, Nokia Shanghai Bell, RAN1#95, Spokane, USA, 12-16 November 2018.
[9] 3GPP. Technical Specification Group Radio Access Network; NR; Physical channels and modulation (Release 17). TS 38.211 V17.5.0, June 2023.
[10] A. Goldsmith. *Wireless Communications*. Cambridge University Press, Stanford University, 1st ed, 2005.
[11] J. G. Proakis, *Digital Communications*, 4th ed. McGraw-Hill, 2001.

[12] B. Singh, Z. Li, O. Tirkkonen, M. A. Uusitalo and P. Mogensen, "Ultra-reliable communication in a factory environment for 5G wireless networks: Link level and deployment study," *IEEE 27th Annual Int. Symposium on Personal, Indoor, and Mobile Radio Communications (PIMRC)*, 2016, pp. 1-5, December 2016.
[13] N. A. Johansson, Y-P. E. Wang, E. Eriksson and M. Hessler, "Radio access for ultra-reliable and low-latency 5G communications," *IEEE Int.l Conf. on Communication Workshop (ICCW)*, pp. 1184-1189, September 2015.
[14] F. Hamidi-Sepehr *et al*., "5G URLLC: Evolution of High-Performance Wireless Networking for Industrial Automation," in *IEEE Communications Standards Magazine*, vol. 5, no. 2, pp. 132-140, June 2021.
[15] 5G CONNI: Private 5G Networks for Connected Industries, "Initial specification and implementation of the building blocks," Deliverable D4.1, March 2021, [Online]. Available: https://5g-conni.eu/wp-content/uploads/2021/03/861459-5G-CONNI-D4.1-Initial-specification-and-implementation-of-the-building-blocks-v1.0.pdf
[16] J. Sachs, G. Wikstrom, T. Dudda, R. Baldemair and K. Kittichokechai, "5G Radio Network Design for Ultra-Reliable Low-Latency Communication," in *IEEE Network*, vol. 32, no. 2, pp. 24-31, March-April 2018.
[17] D. Segura, E J Khatib, J. Munilla and R. Barco, "5G Numerologies Assessment for URLLC in Industrial Communications", *Sensors*, vol. 21, no. 7, pp. 2489, April 2021.
[18] B. Bulut Cebecioglu *et al*., "Sub-6 GHz Channel Modeling and Evaluation in Indoor Industrial Environments," in *IEEE Access*, vol. 10, pp. 127742-127753, December 2022.
[19] 3GPP. NR; Base Station (BS) conformance testing; Part 1: Conducted conformance testing. TS 38.141-1 V18.2.0, June 2023.
[20] M. E. Leinonen, N. Tervo, M. Jokinen, O. Kursu and A. Pärssinen, "5G mm-Wave Link Range Estimation Based on Over-the-Air Measured System EVM Performance," *2019 IEEE MTT-S Int. Microwave Symposium (IMS)*, pp. 476-479, June 2019.
[21] R. Schmogrow *et al*., "Error Vector Magnitude as a Performance Measure for Advanced Modulation Formats," in *IEEE Photonics Technology Letters*, vol. 24, no. 1, pp. 61-63, January 2012.
[22] R. A. Shafik, M. S. Rahman, A. R. Islam and N. S. Ashraf, "On the error vector magnitude as a performance metric and comparative analysis," *2006 Int. Conf. on Emerging Technologies*, pp. 27-31, November 2006.
[23] H. A. Mahmoud and H. Arslan, "Error Vector Magnitude to SNR Conversion for Nondata-Aided Receivers", *IEEE Trans. on Wireless Communications*, Vol.8, Issue.5, pp.2694-2704, May 2009.
[24] K. Ghairabeh, K. Gard, and M. Steer. "Accurate Estimation of Digital Communication System Metrices - SNR, EVM and ρ in a Nonlinear Amplifier Environment". *IEEE Trans. on Communications*, pp.734–739, Sept. 2005.
[25] H. Li and W. Ye, "Study of Digital Modulation Signal Error Vector Magnitude Based on Vector Signal Analyzer," *8th Int. Symposium on Computational Intelligence and Design (ISCID)*, pp. 100-103, December 2015.
[26] R. Hassum, M. Flaherty, R. Matreci, M. Taylor, "Effective Evaluation of Link Quality Using Error Vector Magnitudes Techniques", *Proceedings of Wireless Communication Conf.*, pp. 89-94, August 1997.
[27] H. K. Al-Musawi, W. P. Ng, Z. Ghassemlooy, C. Lu, and N. Lalam, "Experimental analysis of EVM and BER for indoor radio-over-fibre networks using polymer optical fibre," in *Proc. 20th Eur. Conf. Netw. Opt. Commun.*, London, U.K., pp. 1–6, Jun./Jul. 2015.
[28] A. Lipovac, B. Modlic and M. Grgic, "OFDM error floor based EVM estimation," *24th Int. Conf. on Software, Telecommunications and Computer Networks (SoftCOM)*, pp. 1-5, September 2016.
[29] K. Morioka *et al*., "EVM and BER evaluation of C band new Airport surface communication systems," *Int. Workshop on Antenna Technology: Small Antennas, Novel EM Structures and Materials, and Applications (iWAT)*, pp. 242-245, March 2014.
[30] X-H. Tan, T. J. Li, "EVM simulation and analysis in digital transmitter", *The Journal of China Universities of Posts and Telecommunications*, vol.16, no. 6, pp. 43-48, December 2009.
[31] M. Cantero, S. Inca, A. Ramos, M. Fuentes, D. Martín-Sacristán and J. F. Monserrat, "System-Level Performance Evaluation of 5G Use Cases for Industrial Scenarios," in *IEEE Access*, vol. 11, pp. 37778-37789, April 2023.
[32] D. Yang, A. Mahmood, S. A. Hassan and M. Gidlund, "Guest Editorial: Industrial IoT and Sensor Networks in 5G-and-Beyond Wireless Communication," in *IEEE Transactions on Industrial Informatics*, vol. 18, no. 6, pp. 4118-4121, June 2022.
[33] B. Razavi, *RF Microelectronics*, Prentice Hall, Upper Saddle River, NJ, 1998.
[34] 3GPP. Technical Specification Group Radio Access Network; NR; User Equipment (UE) radio transmission and reception; Part 2: Range 2 Standalone (Release 18). TS 38.101-2. V18.2.0, June 2023.
[35] E. I. Adegoke, E. Kampert and M. D. Higgins, "Channel Modeling and Over-the-Air Signal Quality at 3.5 GHz for 5G New Radio", *IEEE Access*, vol. 9, pp. 11183-11193, January 2021.

Berna Bulut Cebecioglu received the B.Sc. degree from Kocaeli University, Kocaeli, Turkey, the M.Sc. and the Ph.D. degrees from the University of Bristol, Bristol, U.K. She worked as a Senior Research Associate in electrical and electronic engineering at the University of Bristol and a Senior Research Fellow at the WMG, the University of Warwick, U.K. She is an Associate Professor in Turkey and currently working as a Senior Research Fellow in future communication systems at Birmingham City University, U.K. Her research interests include B5G and 6G networks, AI/ML, cross-layer design and optimisations of wireless networks, multimedia multicasting and broadcasting, application layer forward error correction codes, propagation modelling, millimetre wave and vehicular communications.

Yuen Kwan Mo has a Ph.D. in communications and network engineering from The University of Warwick, Coventry, UK. He is a Project Engineer with the Connectivity and Communications Technology Research Group, WMG, The University of Warwick. His specialisms include: 5G and cellular communications for Industry 4.0 applications, connected and autonomous vehicles, millimeter-wave communications, massive MIMO, precoding techniques and optimization algorithms.

Son Dinh-Van received a B.S. degree from Hanoi University of Science and Technology, Vietnam, in 2013, the M.S. degree from Soongsil University, Seoul, South Korea, in 2015, and the Ph.D. degree from Queen's University of Belfast, Belfast, UK, in 2019, all in electrical engineering. He is currently a Research Fellow with the Connectivity and Communications Technology Research Group, WMG, The University of Warwick, UK. He was a Data Scientist with Frequenz Gmbh, Germany, and a Visiting Researcher with Middlesex University, London, UK, in 2020 and 2021. His current research interests include 5G-and-beyond communications for manufacturing, wireless security, millimeter-wave, and machine learning.

Alex Evans joined WMG as a Project Engineer in 2017 and has since been promoted to Lead Engineer. During this time he has helped to deliver a number of industry collaborative advanced technology automation, digital manufacturing and data collection projects. Having received a BSc in Cybernetics and Control Engineering from the University of Reading in 1993, the early years of his career were spent designing, building and programming embedded microcontroller projects for a variety of customers in scientific and automation industries. A further 10+ years working for a leading HMI manufacturer and 9 years as a self-employed HMI and PLC software engineer enabled him to gain experience with all the leading PLC technologies, across a variety of sectors including automotive, textiles, food, utilities, building automation and energy monitoring.

De Mi (Senior Member, IEEE) received the B.Eng. degree from the Beijing Institute of Technology, China, the M.Sc. degree from the Imperial College London and the Ph.D. degree from the University of Surrey, U.K. He is currently an Associate Professor in future communication systems and the Head of the Future Information Networks (FINET) Research Cluster with the College of Computing at Birmingham City University. Prior to this, he worked with the Institute for Communication Systems at the University of Surrey. He is also a Visiting Scholar at Shanghai Jiao Tong University, China. His research interests include B5G/6G radio access techniques, radio access network architecture and protocols, hypercomplex signal processing, and the next generation broadcast and multicast communications.

Matthew D. Higgins (Senior Member, IEEE) is a Reader at the University of Warwick, where he leads WMG's Connectivity and Communications Technology Research Group within its Intelligent Vehicles Directorate. His research interests span 5G and Beyond, Core Networking, IEEE 802.3xx, GNSS, and Timing, with applications to both the Automotive and Manufacturing domains. Coupled with an overarching motivation to ensure ongoing resilience of the domain is considered, Matthew leads many high-value collaborative projects funded through EPSRC, Innovate UK, and HVMC, as well as also leading multiple projects funded directly by industry.

Raouf Abozariba (Member, IEEE) received the Ph.D. degree from Staffordshire University in 2017, and was a Senior Research Associate with the School of Computing and Communications, Lancaster University, U.K. He joined Birmingham City University, U.K., in 2019, where he is currently a Senior Lecturer with the College of Computing. He is frequently invited as a reviewer for many prestigious and first-tier journals in communications. He has led large-scale national research projects, such as a £0.26m U.K. project (5GRIT) trialling TV White Space technology to test the potential for shared spectrum radio to deliver 5G services to rural areas. He was a Co-Investigator of the £1m DCMS-funded project, 5GCF, developing and evaluating new sensor technologies over 5G networks in forest environments, leveraging uncrewed vehicles, such as robots and drones. His current research focuses on network QoS evaluation, NOMA technology, dynamic resource allocation, and realtime communication for machine learning tasks and applications.

Professor Adel Aneiba is the Head of the College of Computing at Birmingham City University. He is an experienced academic leader with 20 years of service in industry and academia. Prof. Aneiba received his BSc in Computer Science from the University of Benghazi-Libya in 1997 and his MSc and PhD in Computer Networks from Staffordshire University in England in 2003 and 2008 respectively. Prof. Aneiba is the creator of the Cyber-Physical Systems (CPS) research group at Birmingham City University. This group specialises in software-defined networking (SDN), network function virtualization (NFV), high computing performance (HCP), future networks (5G and LPWAN), AI/ML, blockchain, and trustworthy protocols and systems. Prof. Aneiba is a member of the research bids reviewers at the EU H2020 evaluation panel for their Digital Innovation Hubs (DIH) federation for large-scale adoption of digital technologies by European SMEs, “DigiFed”. He has secured and led several research projects in the area of networking and IoT funded by UKRI worth £1.2M. His research contribution has reached out to and impacted key global challenges such as clean energy and climate change. His CoP26 project was funded by the British Council, Japan sector in partnership with a top global ranking university in Japan (University of Tokyo) and the University of Negeri Gorontalo in Indonesia around Bioenergy using smart sensing technologies and state of the art connectivity and intelligent solutions [5G/IoT/AI/ML].